J Ind Microbiol Biotechnol (2014) 41:1145–1158
DOI 10.1007/s10295-014-1443-2

SIMB
Society for Industrial Microbiology and Biotechnology

Expression, characterization, and improvement of a newly cloned halohydrin dehalogenase from *Agrobacterium tumefaciens* and its application in production of epichlorohydrin

Zhi-Qiang Liu · Ai-Cun Gao · Ya-Jun Wang · Yu-Guo Zheng · Yin-Chu Shen

Received: 12 January 2014 / Accepted: 2 April 2014 / Published online: 29 April 2014

Abstract A gene encoding halohydrin dehalogenase (HHDH) from *Agrobacterium tumefaciens* CCTCC M 87071 was cloned and expressed in *Escherichia coli*. To increase activity and stability of HHDH, 14 amino acid residues around the active site and substrate-binding pocket based on the structural analysis and molecular docking were selected as targets for site-directed mutagenesis. The studies showed that the mutant HHDH (Mut-HHDH) enzyme had a more accessible substrate-binding pocket than the wild-type HHDH (Wt-HHDH). Molecular docking revealed that the distance between the substrate and active site was closer in mutant which improved the catalytic activity. The expressed Wt-HHDH and Mut-HHDH were purified and characterized using 1,3-dichloro-2-propanol (1,3-DCP) as substrates. The specific activity of the mutant was enhanced 26-fold and the value of k_{cat} was 18.4-fold as compared to the Wt-HHDH, respectively. The Mut-HHDH showed threefold extension of half-life at 45 °C than that of Wt-HHDH. Therefore it is possible to add 1,3-DCP concentration up to 100 mM and epichlorohydrin (ECH) was produced at a relatively high conversion and yield (59.6 %) using Mut-HHDH as catalyst. This Mut-HHDH could be a potential candidate for the upscale production of ECH.

Keywords Halohydrin dehalogenase · Site-directed mutagenesis · 1,3-Dichloro-2-propanol · Epichlorohydrin

Z.-Q. Liu · A.-C. Gao · Y.-J. Wang · Y.-G. Zheng (✉) · Y.-C. Shen
Institute of Bioengineering, Zhejiang University of Technology, Hangzhou 310014, Zhejiang, People's Republic of China
e-mail: zhengyg@zjut.edu.cn

Introduction

Currently, biocatalysts are playing an important role in the chemicals industry, especially in the production of chiral substances [3, 6, 33]. Halohydrin dehalogenase (HHDH, EC 4.5.X.X) can catalyze a halohydrin to its corresponding epoxide without any cofactors for keeping its activity [1, 30]. HHDH has been widely used in the epoxide ring opening reaction with the presence of nucleophiles such as cyanide-, azide-, and nitrite ions [13, 19, 20, 21, 23]. It is reported that HHDHs have been found in several microorganisms that utilized halohydrins as carbon and energy sources [2, 29, 32]. In the past few decades, a number of HHDHs have been purified and characterized from *Arthrobacter* sp. strain AD2 [30], *Corynebacterium* sp. strain N-1074 [22, 35], *Arthrobacter erithii* H10a [2], *Arthrobacter* sp. strain PY1 [32], and *Agrobacterium* sp. strain NHG3 [12]. The genes encoding HHDHs have been cloned and expressed and the recombinant HHDHs were characterized in detail [31, 35]. These HHDHs were increasingly recognized as attractive tools for the preparation of bio-pharmaceutical intermediates and biodegradation of various chlorinated environmental pollutants [3, 10, 11, 16, 21, 32].

Epichlorohydrin (ECH) is an important compound widely used as a raw material for the synthesis of epoxy resins in polymer chemistry [23]. ECH is also an intermediate for the synthesis of pheromone anisomycin, propranolol analogs, and β-blockers [17, 19]. HHDH from *A. tumefaciens* can catalyze the dehalogenation of vicinal halohydrins to produce their corresponding epoxides [13, 19]. The nucleotide sequence of this enzyme, three-dimensional (3D) structure, and catalytic mechanism have been previously solved [5, 6, 28, 31]. The HHDH from *A. tumefaciens* shows significant sequence and mechanistic similarity with the short-chain dehydrogenase/reductase

enzyme family. Analysis of the catalytic mechanism showed that Ser132-Tyr145-Arg149 located in a loop-rich cavity was involved as the catalytic triad [5]. The catalytic process by HHDH can be divided into ring closure and ring opening. Tyr145 as the catalytic base firstly takes up a proton from the hydroxyl group adjacent to the chloride atom, and concurrently the substrate oxygen performs a nucleophilic attack on the halogen-bearing carbon atom, resulting in ring closure and liberation of a chloride ion. Second, the nucleophile (CN^-) opens the epoxide ring by nucleophilic attack, while the Tyr145 donates a proton to the oxygen atom of the epoxide ring. Thereby the cyanohydrin is formed rapidly [6, 8, 31]. Recently, the catalytic properties and stability of HHDH have been improved by mutagenesis [9, 26, 27], but it still needs further improvement to fit the desired transformation, which requires high activity and stability in its industrial applications.

The aim of the present study is to construct a novel biocatalyst with high activity and stability, and also to assess its applicability in production of ECH. In this study, the HHDH gene from *A. tumefaciens* CCTCC M 87071 was cloned and expressed in *Escherichia coli*. Based on previous reports and structure analysis of HHDH [9, 26, 27], 14 amino acid residues close to the catalytic center and the halide-binding site were selected to create mutant HHDH (Mut-HHDH) via site-directed mutagenesis. After expression, the wild-type (Wt-HHDH) and Mut-HHDH were purified and characterized to investigate their optimal reaction temperatures and pH, tolerance to metal ions and chemicals, as well as reactions using different halohydrins as substrates. In addition, the potential applications of the Mut-HHDH in the biotransformation of 1,3-dichloro-2-propanol (1,3-DCP) to ECH were investigated.

Materials and methods

Bacterial strains, plasmids, and growth conditions

A. tumefaciens CCTCC M 87071, used for extraction of genomic DNA, was cultivated in nutrient broth containing 5 g/l peptone, 1 g/l meat extract, 2 g/l yeast extract, and 5 g/l NaCl at 30 °C for 12 h [31]. *E. coli* JM109 and *E. coli* BL21 (DE3) were used as hosts for cloning and expression. The plasmid pET-28b(+) was used for overexpression of protein. Cells were incubated at 37 °C in Luria–Bertani (LB) medium (1 % tryptone, 0.5 % yeast extract, and 0.5 % NaCl) containing 50 μg/ml kanamycin (Kan).

Chemicals and enzymes

1-chloro-2-propanol, 1,3-DCP, 2-bromoethanol, 1-bromo-2-propanol 1,3-dibromo-2-propanol and 2,3-dichloro-1-propanol (2,3-DCP) were purchased from J&K Scientific Ltd (Shanghai, China). *pfu* DNA polymerase, T4 DNA ligase, and restriction endonuclease including *Nco*I and *Xho*I, were purchased from Fermentas International Inc (Shenzhen, China). PrimeSTAR HS DNA Polymerase for site-directed mutagenesis was purchased from Takara (Dalian, China). All other chemicals used were of analytical reagent grade.

Gene manipulation

Genomic DNA from *A. tumefaciens* CCTCC M 87071 was prepared as described by Sambrook et al. [24]. Plasmid DNA was isolated using the AxyPrep Plasmid Miniprep Kit (Axygene Biotech Ltd., Hangzhou, China) according to the instructions of the manufacturer. Extraction of DNA from agarose gel was carried out with the AxyPrep DNA Gel Extraction Kit (Axygene Biotech Ltd.).

Cloning of HHDH gene

The HHDH gene was amplified by polymerase chain reaction (PCR) using genomic DNA of *A. tumefaciens* CCTCC M 87071 as template [24]. Based on the amino acid sequence of HHDH from *A. tumefaciens,* the oligonucleotide primers, P1: 5′-AGGCCATGGGTTCAACCG CAATTGTA ACAAAC-3′, and P2: 5′-AATCTCGAGC TACTCGGGCATACCAGGCCAAC-3′ were designed. The restriction sites *Nco*I and *Xho*I were introduced into the primers (underlined parts). The PCR reaction system (50 μl) consisted of 50 ng genomic DNA, 50 μM each dNTP, 0.5 μM P1 and P2, 5 μl 10× *pfu* DNA buffer and 2 U *pfu* DNA polymerase. Amplification was carried out in a thermal cycler (Bio-Rad, Hercules, CA, USA) under the following conditions: 5 min at 95 °C, 35 cycles of 30 s at 95 °C, 30 s at 55 °C, 1 min at 72 °C and one final step of 10 min at 72 °C. The PCR product was digested with *Nco*I and *Xho*I, and then ligated into the *Nco*I- and *Xho*I-linearized expression vector pET-28b to construct the recombinant plasmid, pET-28b-HHDH. Subsequently, the recombinant plasmid pET-28b-HHDH was introduced into *E. coli* JM109 using heatshock method [4].

Site-directed mutagenesis

The recombinant plasmid pET-28b-HHDH extracted from *E. coli* JM109 cells was used as template for mutagenesis. The position of amino acid substitution and synthetic mutagenic forward and reverse primers were shown in Table 1. The mutated plasmids from the previous round of mutation were used as template for next mutation. The mutagenesis PCR was performed with PrimeSTAR HS DNA Polymerase using a program of 5 min at 95 °C followed by 30

Table 1 Sequences of oligonucleotides used for site-directed mutagenesis

Position of amino acid substitution	Mutation primer sequence
Q37H	F: 5′-GAAAGCTTCAAACACAAGGACGAACTTG-3′ R: 5′-CAAGTTCGTCCTTGTGTTTGAAGCTTTC-3′
Y70F	F: 5′-CAGTTACCTCCGCTTTCGGTCAAGTTGATG-3′ R: 5′-CATCAACTTGACCGAAAGCGGAGGTAACTG-3′
P84L, Q87R	F: 5′-GACATATTCGCACTGGAGTTCCGTCCCATAGATAAATAC-3′ R: 5′-GTATTTATCTATGGGACGGAACTCCAGTGCGAATATGTC-3′
T131A, T134A	F: 5′-ATATTATCTTTATTGCGTCTGCAGCGCCCTTCGGGCC-3′ R: 5′-GGCCCGAAGGGCGCTGCAGACGCAATAAAGATAATAT-3′
T144A, T146S	F: 5′-GGAAGGAACTTTCTGCGTACAGCTCAGCCCGAGCAGGTG-3′ R: 5′-CACCTGCTCGGGCTGAGCTGTACGCAGAAAGTTCCTTCC-3′
C153S, T154A	F: 5′-AGCAGGTGCAAGCGCGTTGGCAAATGCCCTTTC-3′ R: 5′-GAAAGGGCATTTGCCAACGCGCTTGCACCTGCT-3′
F186Y	F: 5′-GAAGATAGTCCCTACTACTACCCCACAGAACCG-3′ R: 5′-CGGTTCTGTGGGGTAGTAGTAGGGACTATCTTC-3′
T194I	F: 5′-ACAGAACCGTGGAAAATCAATCCAGAACACGTTGCCC-3′ R: 5′-GGGCAACGTGTTCTGGATTGATTTTCCACGGTTCTGT-3′
M245V, W249A	F:5 ′-GGCGGATTCCCAGTGATCGAGCGTGCGCCTGGTATGCC-3′ R: 5′-GGCATACCAGGCGCACGCTCGATCACTGGGAATCCGCC-3′

The *underlined sections* indicate the mutagenized nucleotides

cycles of 95 °C for 40 s, 55 °C for 20 s, 72 °C for 8 min and a final extension at 72 °C for 10 min. The restriction enzyme *Dpn*I was added to the PCR products directly to remove the methylated template for 1 h at 37 °C in each round. Then the products were purified and transformed into *E. coli* BL21 (DE3) for expression.

The recombinant Wt-HHDH and Mut-HHDH were grown at 37 °C in 50 ml of LB medium with Kan (50 μg/ml) and to optical density (OD) with 600 nm between 0.6 and 1.0. Isopropyl-β-D-1-thiogalactopyranoside (IPTG) was added to the culture at a final concentration of 0.5 mM to induce the expression of the Wt-HHDH and Mut-HHDH. The cultures were then further grown for 8 h at 28 °C. Afterwards, the induced cells were harvested via centrifugation at 12,000×*g* for 10 min.

Scale-up of Wt-HHDH and Mut-HHDH production in a bioreactor

Cultivation was performed in a 500-l mechanically stirred tank bioreactor (Baoxing Biotech Company, Shanghai, China). The recombinant Wt-HHDH and Mut-HHDH cultures (300 ml) were transferred into a 50-l bioreactor that contained 30 l × LB medium with Kan (50 μg/ml) and then incubated at 37 °C for 4 h, respectively. The inoculums were transferred into a 500-l bioreactor that contained 300 l of cultivation medium (12 g/l yeast extract, 15 g/l tryptone, 10 g/l NaCl, 15 g/l glycerol, 5 g/l $(NH_4)_2SO_4$ and 1.36 g/l KH_2PO_4) with Kan (50 μg/ml) and grown at 37 °C. When OD_{600} reached between 4.5 and 5.0, the lactose was added with a final concentration of 1.5 % (w/v) to induce expression of the Wt-HHDH and Mut-HHDH for 8 h at 28 °C. Cells were collected by centrifugation at 4 °C, 4,000×*g* for 20 min, and stored at −20 °C until use.

Purification of Wt-HHDH and Mut-HHDH

The recombinant Wt-HHDH and Mut-HHDH cells (5 g) were suspended in 50 ml 20 mM phosphate buffer (pH 8.0) and disrupted for 30 min using an ultrasonic oscillator. The cell debris was removed via centrifugation at 12,000 × *g* for 30 min. The supernatant solutions were used as the cell extract. A column (1 × 10 cm^2) containing Ni-chelating Sepharose was preconditioned with buffer A (20 mM NaH_2PO_4–Na_2HPO_4, 500 mM NaCl, and 20 mM imidazole; pH 8.0) for 10 min. The cell extract was then flowed into the column for 15 min at a flow rate of 2 ml/min. The column was washed with buffer A to remove unbound proteins. The protein sample was successively eluted using a step gradient of buffer B (20 mM NaH_2PO_4–Na_2HPO_4, 500 mM NaCl, and 500 mM imidazole; pH 8.0) for 15 min at a flow rate of 5 ml/min. The enzyme solution was dialyzed overnight in ice with 20 mM sodium phosphate (pH 8.0). The resulting enzyme was stored at 4 °C.

Protein analysis

Sodium dodecyl sulfate–polyacrylamide gel electrophoresis (SDS–PAGE) analysis was carried out with a 5 % acrylamide stacking gel (pH 6.8) and 12 % separating gel (pH 8.8) as described by Laemmli [18]. Samples were mixed with 2× loading buffer and heated at 100 °C for 10 min before electrophoresis. The gel was stained with 0.1 % Coomassie brilliant blue R-250 for detection of

proteins, and then destained with 10 % ethanol and 10 % acetic acid solution. A wide molecular range (10–170 kDa) protein standard was used as molecular mass marker.

Protein concentration

The protein concentration was quantified by using the bicinchoninic acid (BCA) protein assay kit (Nanjing Keygen Biotechnology Co, Nanjing, China) based on the method of Smith et al. [25]. The assay was carried out according to the manufacturer's instructions incubating samples for 30 min at 37 °C, and then the absorbance at 562 nm was determined.

Activity assay

The Wt-HHDH and Mut-HHDH activities were determined by measuring the amount of ECH from 1,3-DCP. The Wt-HHDH reaction mixture consisted of 0.2 M of Na_2HPO_4–NaH_2PO_4 buffer (pH 7.5), 40 mM 1,3-DCP and 26.4 mg/l purified Wt-HHDH with a final volume of 1 ml, at 40 °C for 8 min and then 20 μl of 2 M H_2SO_4 was added to terminate the reaction.

The Mut-HHDH reaction mixture consisted of 0.2 M of Na_2HPO_4–NaH_2PO_4 buffer (pH 7.5), 40 mM 1, 3-DCP, and 4.2 mg/l purified Mut-HHDH with a final volume of 1 ml, at 40 °C for 3 min and then 20 μl 2 M H_2SO_4 was added to terminate the reaction.

The ECH concentration was determined using a GC-7890A system equipped with a HP-5 capillary column (30 m × 0.32 mm, 0.25-μm film thickness) fitted with a flame ionization (FID) detector. Nitrogen was used as carrier gas at a flow rate of 1.0 ml/min. The column temperature was set at 80 °C to keep 4 min then 10 °C/min heating to 100 °C and the inlet and detector temperatures were 230 and 250 °C, respectively. The retention times of 1,3-DCP and ECH were 3.0 min and 4.8 min, respectively. One unit (U) of activity is defined as the amount of enzyme that produces 1 mM of ECH per minute.

Characterization of the purified Wt-HHDH and Mut-HHDH

Optimum temperature and stability of purified Wt-HHDH and Mut-HHDH

The optimum temperatures of Wt-HHDH and Mut-HHDH were determined by incubating the enzyme in assay mixtures at temperatures ranging from 30 to 75 °C and determining the residual enzyme activities in 0.2 mM of Na_2HPO_4–NaH_2PO_4 buffer (pH 7.5), respectively. For thermostability analysis, triplicate samples of Wt-HHDH and Mut-HHDH were incubated for 400 min at temperatures ranging from 40 to 55 °C. The residual activity was determined at 40 °C under the standard assay conditions. The non-heated enzyme was taken as the control (100 % activity).

Optimum pH and stability of purified Wt-HHDH and Mut-HHDH

The optimum pHs for Wt-HHDH and Mut-HHDH activity were determined using the following buffers: 0.2 M Na_2HPO_4–NaH_2PO_4 (pH 6.5–8.0), 0.2 M $Na_2B_4O_7$–H_2BO_3 (pH 8.0–9.0), and 0.2 M Gly–NaOH (pH 9.0–10.0) and determining the enzyme activities in 40 °C, respectively. To determine the pH stability, the purified enzymes were pre-incubated in different buffers of Na_2HPO_4–NaH_2PO_4 (pH 7.5–8.0) and $Na_2B_4O_7$–H_2BO_3 (pH 8.0–8.4) with the concentration of 0.2 M at 0 °C for 65 h. The residual activities were quantified under the standard assay conditions.

Effect of metal ions and chemicals on enzyme activity

Various metal ions and chemicals were added to the enzymatic preparations and pre-incubated for 30 min at 30 °C. The effects of metal ions on enzyme activities were studied by incubating the enzyme in reaction mixtures with different metal ions including Al^{3+}, Fe^{3+}, Fe^{2+}, Mg^{2+}, Zn^{2+}, Ca^{2+}, Mn^{2+}, Cu^{2+}, and Ag^{+} with a final concentration of 1 and 5 mM. The effects of chemicals on enzyme activity were studied by incubating the enzyme in reaction mixtures with different chemicals including Tween-20, Tween-80, Triton X-100, and SDS with a final concentration of 1 and 5 %, and the final concentration of EDTA was 1 and 10 mM. The residual activity was measured under standard assay conditions and expressed as a percentage of the activity observed in the absence of any additive.

Substrate specificity and kinetic analysis

The substrate specificities of Wt-HHDH and Mut-HHDH were determined by replacing 1,3-DCP in the assay mixture with 1-chloro-2-propanol, 1,3-dibromo-2-propanol, 2,3-DCP, 2-bromoethanol and 1-bromo-2-propanol with the concentration of 40 mM, respectively. The activity was measured under standard assay condition. Kinetic parameters of Wt-HHDH and Mut-HHDH were calculated from the initial rate activities of the purified enzyme using 1,3-DCP and 2,3-DCP as substrates at the concentrations ranging from 10 to 200 mM and the activity was measured under the standard assay conditions. The initial rate obtained was fitted to the equation: $V = V_{max} \times [S]/(K_m + [S])$, where V_{max} is the maximum rate, (S) is substrate concentration, and K_m is the Michaelis constant. All the experiments were repeated in triplicate if not specifically noted.

Modeling and molecular docking

The 3D structure of Wt-HHDH form *A. tumefaciens* (PDB code: 1PWX) was obtained from PDB database [5], and used as the template to generate a model structure for Mut-HHDH by Build Homology Models (MODELER) in Discovery Studio 2.1 (Accelrys Software, San Diego, CA, USA). The generated structures were improved by subsequent refinement of the loop conformations by assessing the compatibility of an amino acid sequence to known PDB structures using the protein health module in DS 2.1. Molecular docking was also performed using the dock ligands module (LibDock) in DS 2.1. 1,3-DCP was docked into the active cavities of the Wt-HHDH and Mut-HHDH, respectively. All protein structure figures were prepared with PyMOL (http://www.pymol.org) [7].

Statistical analysis

All experiments in this study were performed in triplicate if not specifically noted. Analysis of variance (ANOVA) was performed with the SAS program version 8.1 (SAS Institute Inc., Cary, NC, USA). The results are expressed as mean ± standard deviation (SD) and the least significant differences for comparison of means were computed at $p < 0.05$.

Results

Mutation design and selection

Studies on the 3D structure and catalytic mechanism of HHDH revealed that the catalytic residues including Ser132, Tyr145, and Arg149 are highly conserved [5, 31]. The halide-binding site was mainly formed by the residues 175–178, and stabilized by Phe12, Asp80, Ser180, Tyr185, Phe186, Tyr187, and Trp249 from other subunits [5, 26]. In addition to the residues mentioned above, Thr134 and Trp139 interact with the substrate directly [9]. Single mutations have shown that disruption of two hydrogen bonds around the halide-binding site increases the release rate of halide, which enhances the overall catalytic activity of the enzyme [26], and all three cysteine residues, Cys30, Cys153, and Cys229, in HHDH have affected the stability of the enzyme by intramolecular disulfide bond formation [27].

Our strategy to improve catalytic efficiency of HHDH was to expand the substrate-binding pocket and increase its binding ability toward the substrates, especially 1,3-DCP, by introducing small, hydrophobic amino acids into HHDH by site-directed mutagenesis at the positions around the active site. Speeded-up the release rate of halide was also considered so that some amino acids close to the halide-binding site residues were semi-randomly selected for mutation. In addition, to improve the stability of HHDH, the formation of intramolecular disulfide bonds was avoided. Based on the analysis above, we chose the following 14 residues to be mutated: Gln37, Tyr70, Pro84, Gln87, Thr131, Thr134, Thr144, Thr146, Cys153, Thr154, Phe186, Thr194, Met245, and Trp249. Figure 1 shows the 3D structure of HHDH, and the positions of mutations are displayed.

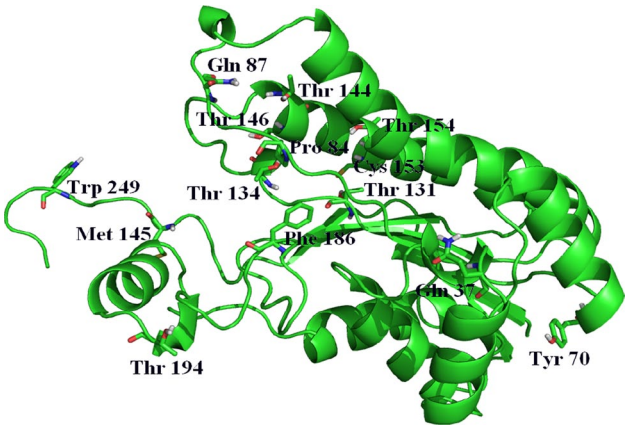

Fig. 1 The 3D structure of Mut-HHDH. The structure is generated based on the reported HHDH from Protein Data Bank (number: 1PWX). α-Helices are represented as *red*, β-strands as *yellow*, and loops as *green*. Residues subjected to mutation are displayed by sphere (color figure online)

The 3D structural analysis and molecular docking

The 3D structure of the mutant HHDH was derived using the DS 2.1 program using Wt-HHDH as the template. Figure 2 displays the structure analysis of Wt-HHDH and Mut-HHDH. The substrate-binding pocket is much more open in Mut-HHDH than that in Wt-HHDH. Molecular docking was further carried out and tried to deeply understand the interactions between 1,3-DCP and the amino acid residues in the active site (Fig. 3). The results showed that 1,3-DCP was successfully docked into each active site of the two enzymes with different free energy of binding, 4.31 and 4.87 kcal/mol for Wt-HHDH and Mut-HHDH, respectively. Moreover, the mutations reduce the distance between the hydroxyl of 1,3-DCP and Tyr145 of the active site, from 2.36 to 1.91 Å. Meanwhile, the distance between the same hydroxyl and Ser132 was also reduced from 2.84 to 2.05 Å.

Cloning and mutagenesis of HHDH gene

A primer set based on the amino acid sequence (GenBank accession no. AAK92099) was used to clone the Wt-HHDH

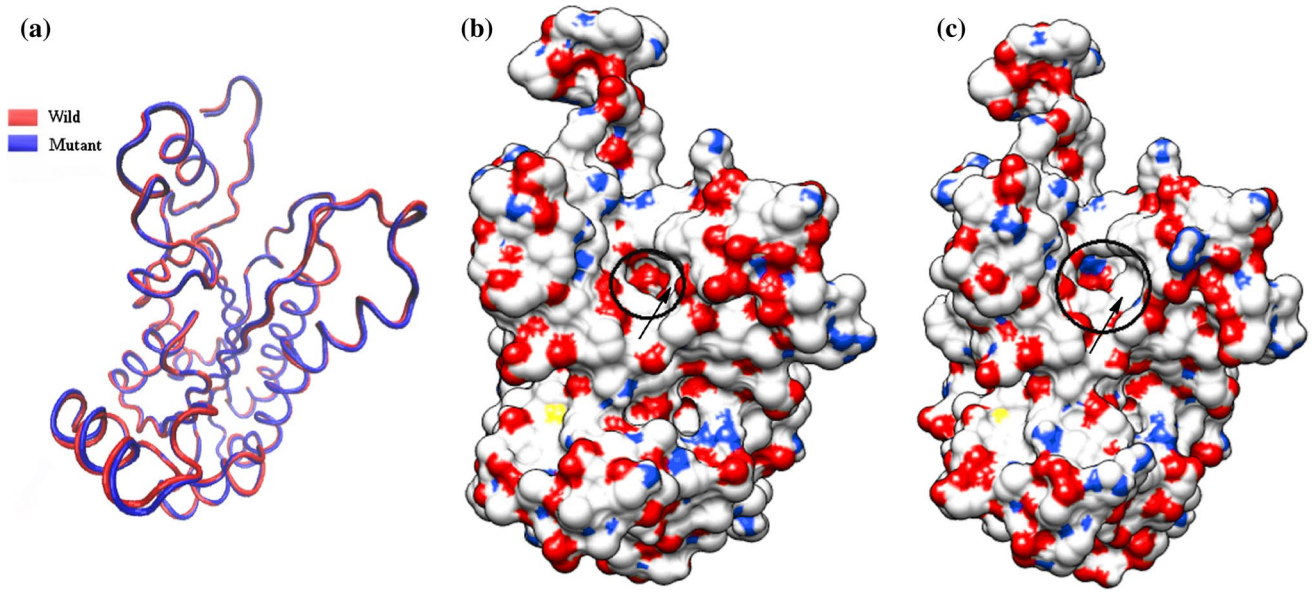

Fig. 2 Structure analysis of Wt-HHDH and Mut-HHDH. **a** Structure alignment of Wt-HHDH and Mut-HHDH, **b** surface representation of Wt-HHDH, **c** surface representation of Mut-HHDH. The active pocket of Mut-HHDH was larger than the Wt-HHDH, which is highlighted with an *arrow* and a *circle* (color figure online)

gene from strain *A. tumefaciens* CCTCC M 87071. The sequenced results of PCR products with primers P1 and P2 showed that the gene fragment consisted of 762 bp, encoding a polypeptide of 254 amino acids with a predicted mass of 27.9 kDa. It was consistent with the HHDH gene reported previously [31], which indicated that the Wt-HHDH gene was successfully cloned. The PCR products were then digested with the appropriate restriction endonuclease and subcloned into an expression vector pET-28b(+). The candidate residues for amino acid substitution of HHDH were selected as shown in Table 1, and each mutation was introduced additively on the HHDH gene cloned on pET-28b(+). The target residues that located adjacently were mutated at one time. Finally, the recombinant plasmid coding the Mut-HHDH carrying 14 amino acid residues was constructed.

Production and purification of Wt-HHDH and Mut-HHDH

The genes encoding the Wt-HHDH and Mut-HHDH were expressed under the control of the T7 promoter in *E. coli* BL21 (DE3), respectively. After being cultured for 2 h, the biomass has an exponential increase for both of Wt-HHDH and Mut-HHDH. The biomass and enzyme activity reaches maximums at 8 and 10 h after induced by lactose, respectively. After completion of the cultivation, the biomass reached 13.3 g(DCW)/l and activity reached 7,459 U/l for Mut-HHDH. However, the biomass reached 11.5 g(DCW)/l and activity reached 216 U/l for Wt-HHDH.

In the constructed expression system in this study, the Wt-HHDH and Mut-HHDH protein with his tags can bind with the Ni–NTA column. After elution with a column buffer containing 500 mM imidazole, the recombinant Wt-HHDH and Mut-HHDH protein was purified through Ni–NTA affinity chromatography after the cell disruption through sonication. SDS–PAGE analysis (Fig. 4) clearly shows the purified Mut-HHDH in lane 2 with a molecular mass of approximate 28 kDa, which is agreement with Wt-HHDH in lane 4. Table 2 summarizes the results of the purification efficiency for Wt-HHDH and Mut-HHDH. The yields of purified Wt-HHDH and Mut-HHDH were 41.1 and 40.9 % and the specific activities were 22 and 582 U/mg, respectively. The pure enzymes were then used to investigate the biochemical characterizations.

Effects of temperatures on the activities and stabilities of Wt-HHDH and Mut-HHDH

Temperature is an important factor that greatly affects the activity and stability of an enzyme. The Wt-HHDH and Mut-HHDH showed the maximum activities at 55 and 65 °C, respectively (Fig. 5a). Retained more than 85 % of its peak activity in the temperature range 50–60 °C of Wt-HHDH and retained more than 90 % of its peak activity in the temperature range 50–70 °C of Mut-HHDH. The activity decreased sharply when the temperature of the reaction system increased. At 75 °C, the purified Wt-HHDH exhibited no activity, and at 85 °C, the Mut-HHDH exhibited no activity.

The thermal stability of the Wt-HHDH and Mut-HHDH is depicted in Fig. 5b. The purified Wt-HHDH could retain almost 80 % of its activity when incubated at 45 °C for

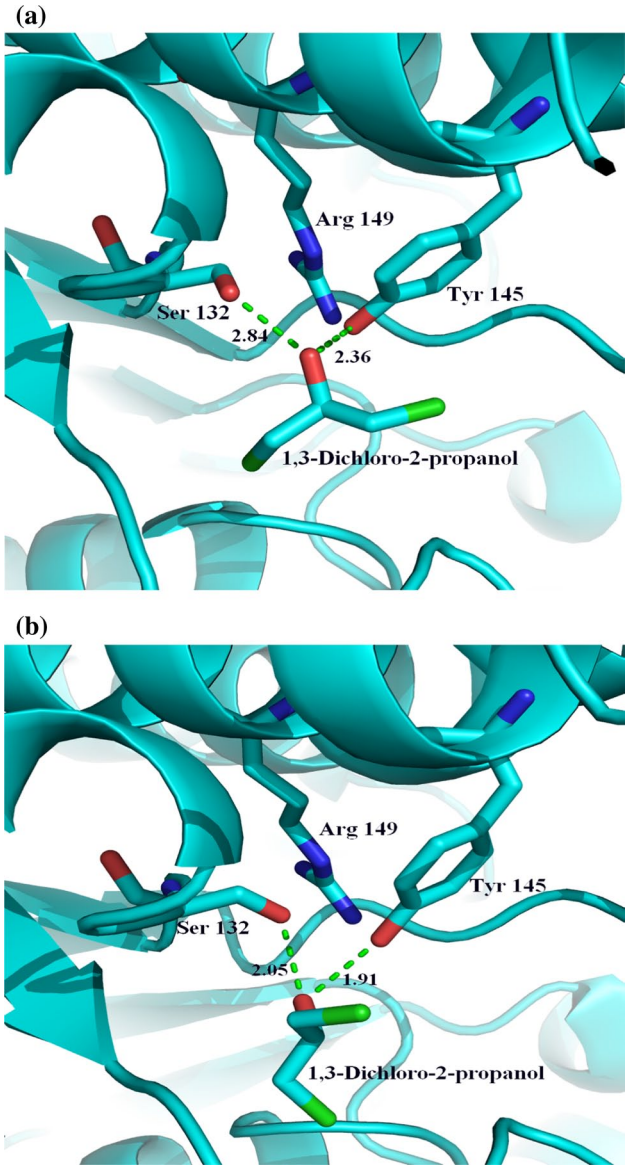

Fig. 3 Docking of 1,3-DCP into the active site of HHDH. **a** Wt-HHDH, **b** Mut-HHDH (color figure online)

120 min and the purified Mut-HHDH could retain almost 95 % of its activity at the same conditions. The half-lives of Wt-HHDH were 33.5, 13.2, 4.8, and 0.84 h at 40, 45, 50, and 55 °C. However, the half-lives of Mut-HHDH were 47.8, 39.2, 32.1, and 14.3 h at 40, 45, 50, and 55 °C, respectively.

Effect of pH on the activities and stabilities of Wt-HHDH and Mut-HHDH

The Wt-HHDH and Mut-HHDH activities were monitored at different pH from 6.5 to 10.0. The optimal pHs for Wt-HHDH and Mut-HHDH were 8.0 and 8.4, respectively (Fig. 6a). The pH stability profile showed that Mut-HHDH is more stable than Wt-HHDH, and more than 82.1 % of its original activity

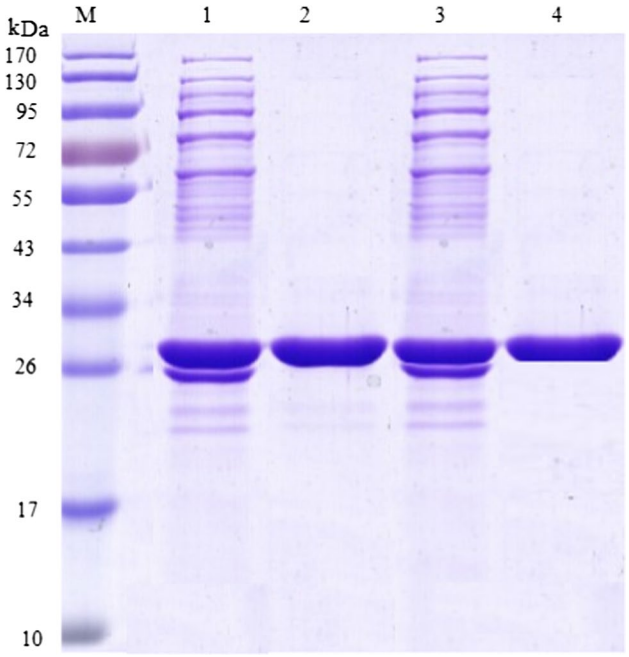

Fig. 4 SDS–PAGE analysis of purified Wt-HHDH and Mut-HHDH. *Lane M* standard proteins marker of different molecular weights, *lane 1* crude Mut-HHDH, *lane 2* purified Mut-HHDH, *lane 3* crude Wt-HHDH, and *lane 4* purified Wt-HHDH (color figure online)

was maintained when exposed at pH levels between 7.5 and 8.4 for 65 h at 0 °C, However, the Wt-HHDH activity was reduced to 30 % at the same conditions (Fig. 6b).

Effect of metal ions and chemicals on Wt-HHDH and Mut-HHDH activities

The effects of various metal ions on the activities of Wt-HHDH and Mut-HHDH are shown in Table 3. There was no significant inhibition on both of them by most of the studied metal ions, when the concentration of added ion was kept at 1 mM. With the additives at a final concentration of 5 mM, the Mut-HHDH activity was slightly promoted by Mn^{2+} and Fe^{2+}, while Al^{3+} and Ag^{+} showed around 11 % loss in activity.

The effects of surfactants on activities of Wt-HHDH and Mut-HHDH are presented in Table 4. Most of the surfactants had little influence on enzyme activities. In the presence of 5 % Tween-20 and Triton X-100, the enzyme retained 90.5 and 89.3 % of their activities, respectively. However, the activities of enzymes were strongly inhibited by SDS. SDS is an ionic detergent with a long hydrophobic tail that binds to the hydrophobic side chains of amino acids. This inhibition may be the result of the changing of the microenvironment of tyrosine and tryptophan groups of enzyme by SDS. The metal chelator EDTA also slightly inhibited the enzyme activities, which indicated that HHDH is not a metalloenzyme.

Table 2 Summary of the purification of Wt-HHDH and Mut-HHDH

Purification step	Total protein (mg)	Total activity (U)	Specific activity (U/mg)	Purification (fold)	Yield (%)
Crude Mut-HHDH	922.5	58,117.5	63.0	1.0	100.0
Purified Mut-HHDH	40.8	23,745.6	582.0	9.2	40.9
Crude Wt-HHDH	579.4	2,607.3	4.5	1.0	100.0
Purified Wt-HHDH	40.7	895.4	22.0	4.9	41.1

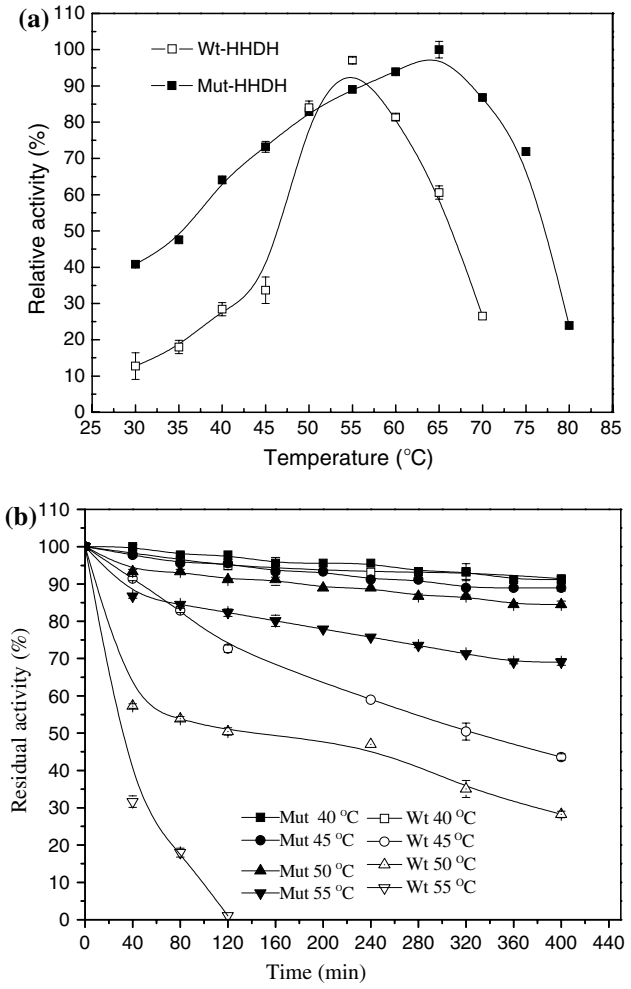

Fig. 5 Effect of temperature on Wt-HHDH and Mut-HHDH. **a** Activity, **b** thermostability. For activity, the temperatures were 30–75 °C. For thermostability analysis, Wt-HHDH and Mut-HHDH were incubated for 400 min at temperatures 40–55 °C. The residual activity was determined under the standard assay conditions

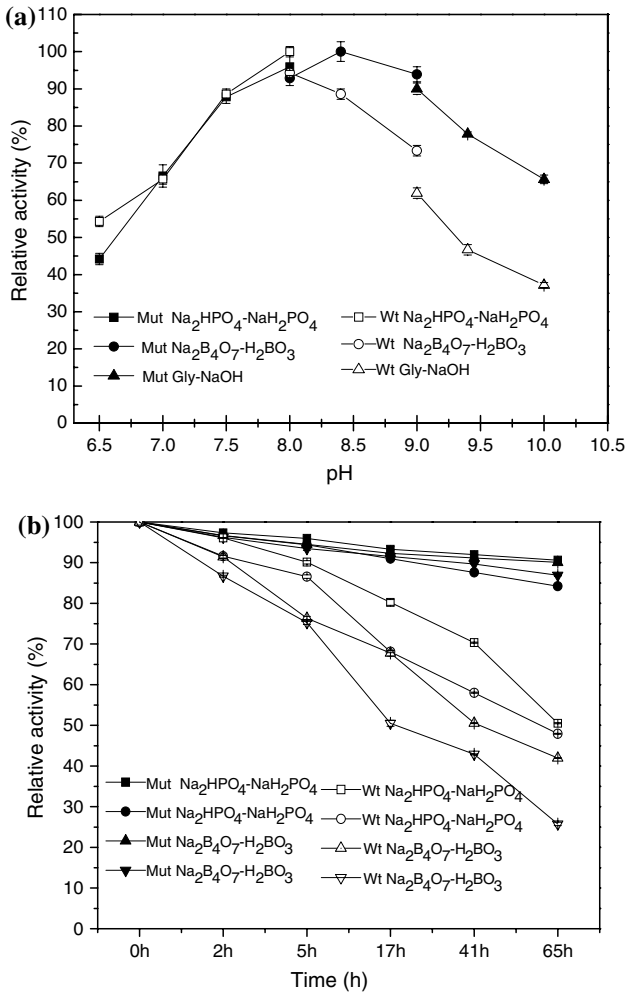

Fig. 6 Effect of pH on Wt-HHDH and Mut-HHDH. **a** Activity, **b** pH stability. For activity, the buffers were 0.2 M Na_2HPO_4–NaH_2PO_4 (pH 6.5–8.0), 0.2 M $Na_2B_4O_7$–H_2BO_3 (pH 8.0–9.0), and 0.2 M Gly–NaOH (pH 9.0–10.0). For pH stability, the purified enzymes were pre-incubated in different buffers of Na_2HPO_4–NaH_2PO_4 (pH 7.5–8.0) and $Na_2B_4O_7$–H_2BO_3 (pH 8.0–8.4) with the concentration of 0.2 M at 0 °C for 65 h. The residual activities were quantified under standard assay conditions

Substrate specificity and catalytic properties

The utility of enzymes often depends on their substrate specificities due to their ability to discriminate among different substrates. The activities of the purified Wt-HHDH and Mut-HHDH towards various substrates are summarized in Table 5. In all cases, halide production rates were much higher with brominated substrates than chlorinated analogs. The chlorinated alcohols tested in this study showed that the 1,3-DCP was the best substrate for Wt-HHDH and Mut-HHDH. The kinetic behaviors of the Wt-HHDH and Mut-HHDH with 1,3-DCP were reasonably well described

Table 3 Effects of metal ions on the activity of Wt-HHDH and Mut-HHDH

Metal ions	Concentration (v/v), mM	Relative activity (%)[a]	Relative activity (%)[b]
Control	–	100.0	100.0
Al^{3+}	1	100.0 ± 0.74	95.4 ± 0.13
	5	96.1 ± 0.86	89.3 ± 1.81
Fe^{3+}	1	105.7 ± 1.21	100.0 ± 0.32
	5	100.0 ± 0.72	96.9 ± 0.64
Fe^{2+}	1	106.6 ± 0.65	103.8 ± 0.09
	5	94.1 ± 0.94	109.9 ± 0.81
Mg^{2+}	1	103.8 ± 0.81	98.4 ± 1.62
	5	101.9 ± 0.36	97.7 ± 1.53
Zn^{2+}	1	92.3 ± 1.38	101.5 ± 2.83
	5	94.1 ± 0.63	92.3 ± 0.92
Ca^{2+}	1	105.2 ± 0.22	98.4 ± 1.62
	5	101.6 ± 0.36	95.5 ± 0.53
Mn^{2+}	1	92.3 ± 0.85	103.8 ± 1.09
	5	98.0 ± 0.94	109.1 ± 0.81
Cu^{2+}	1	109.52 ± 0.18	99.2 ± 0.81
	5	96.1 ± 1.81	94.6 ± 0.09
Ag^{+}	1	96.1 ± 1.93	98.6 ± 1.67
	5	98.0 ± 0.90	75.6 ± 1.13

The activity was measured under standard assay conditions

[a] Relative activity of Wt-HHDH

[b] Relative activity of Mut-HHDH

Table 4 Effects of surfactants and inhibitors on the activity of Wt-HHDH and Mut-HHDH

Surfactants	Concentration (v/v)	Relative activity (%)[a]	Relative activity (%)[b]
Control	–	100.0	100.0
Tween-20	1 %	101.1 ± 1.51	71.1 ± 0.53
	5 %	95.5 ± 0.51	90.5 ± 0.54
Tween-80	1 %	95.6 ± 0.52	105.6 ± 0.57
	5 %	93.4 ± 1.16	97.4 ± 1.19
Triton X-100	1 %	98.3 ± 2.10	88.9 ± 3.85
	5 %	99.3 ± 0.55	89.3 ± 0.13
SDS	1 % (w/v)	56.0 ± 1.26	40.0 ± 4.03
SDS	5 % (w/v)	0.0	0.0
EDTA	1 mM	88.6 ± 1.26	89.6 ± 2.93
	10 mM	82.2 ± 0.62	89.2 ± 0.12

The activity was measured under standard assay conditions

[a] Relative activity of Wt-HHDH

[b] Relative activity of Mut-HHDH

by the Michaelis–Menten model (Fig. 7). The K_m, V_{max}, k_{cat}, and k_{cat}/K_m values of purified enzymes against these compounds are shown in Table 6. From the analysis of the K_{cat} values, the Mut-HHDH (k_{cat} = 1,011.1/s) showed higher catalytic efficiency toward 1,3-DCP compared to Wt-HHDH (k_{cat} = 54.9/s), which allowed application of this enzyme in the production of ECH in large scale.

Table 5 Substrate specificity of Wt-HHDH and Mut-HHDH

Substrate	Relative activity (%)[a]	Relative activity (%)[b]
1,3-DCP	100.0	100.0
2,3-DCP	28.3	46.3
1,3-Dibromo-2-propanol	113.2	122.9
1-Chloro-2-propanol	88.4	97.1
1-Bromo-2-propanol	168.5	220.8
2-Bromoethanol	55.4	61.6

The concentration of each substrate was 40 mM. The activity was measured under standard assay conditions

[a] Relative activity of Wt-HHDH

[b] Relative activity of Mut-HHDH

Effect of temperature on stability of ECH

The ECH is unstable and self-hydrolysis will be happened at higher temperatures, the stabilities of ECH at different temperatures were investigated. The effect of temperature on stability of ECH is depicted in Fig. 8. About 87.1 and 80.2 % of ECH remained after 60 min of incubation at 40 and 45 °C, respectively. However, the concentration of ECH only reached 59.7 % after 60 min of incubation at 50 °C. To reduce the spontaneous hydrolysis of ECH, the reaction was performed at a temperature of 45 °C.

Synthesis of ECH by Wt-HHDH and Mut-HHDH

Synthesis of ECH from 1,3-DCP was carried out using Wt-HHDH and Mut-HHDH as biocatalysts. The Wt-HHDH reaction mixture consisted of 0.2 M of Na_2HPO_4–NaH_2PO_4 buffer (pH 8.0), 30 mM 1,3-DCP and 21.1 mg/l Wt-HHDH with a final volume of 10 ml in a 50-ml flask. The reaction proceeded for 1 h at 45 °C with stirring. The Mut-HHDH reaction mixture consisted of 0.2 M $Na_2B_4O_7$–H_2BO_3 (pH 8.4), 100 mM 1,3-DCP, and 3.8 mg/l Mut-HHDH with a final volume of 10 ml in a 50-ml flask. The reactions proceeded for 1.5 h at 45 °C with stirring.

The time course of the synthesis of ECH using the Wt-HHDH as catalyst was shown in Fig. 9a. ECH was produced with a molar yield of 35.3 % within 50 min. When the reaction time extended to 60 min, 1,3-DCP was consumed 58.5 %, while yield of ECH reduced to 28.9 % and continuously decreased upon prolonged incubation. The time course of the transformation of 1,3-DCP to ECH using

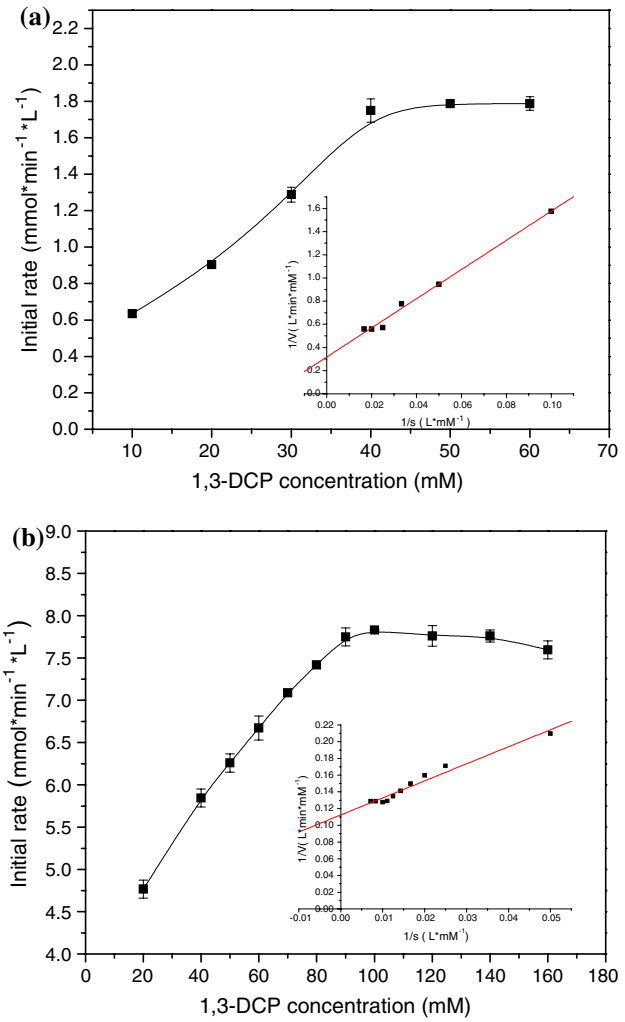

Fig. 7 Initial rate of at different 1,3-DCP concentrations. **a** Wt-HHDH, **b** Mut-HHDH. The concentration of using 1,3-DCP as substrates at ranging from 10 to 200 mM and the activity was measured under the standard assay conditions (color figure online)

Mut-HHDH as catalyst (Fig. 9b) showed that ECH was produced with a molar yield of 59.6 % (59.6 mM) within 1 h. When the reaction time extended to 1.5 h, 1,3-DCP was consumed 67.4 %, while yield of ECH reduced to 54.3 %. Because the HHDH can catalyze the ring closure of 1,3-DCP to ECH, as well as the ring opening of ECH to 1,3-DCP in the presence of Cl^-, which is the main reason that the 1,3-DCP could not be converted completely and the yield of ECH was always low in aqueous phase.

Analysis of ECH by complexation gas chromatography and gas chromatography-mass spectrometry

The gas chromatography spectrum revealed that the product was (±)-ECH. The retention times of (*S*)-ECH and (*R*)-ECH were 4.4 and 4.5 min, respectively

Table 6 Kinetic constants of Wt-HHDH and Mut-HHDH on different substrate

Enzyme	Substrate	V_{max} (mM/min)	K_m (mM)	K_{cat} (/s)	k_{cat}/K_m (/mM/s)
Wt-HHDH	1,3-DCP	3.1	39.3	54.9	1.4
	2,3-DCP	2.0	47.1	24.8	0.5
Mut-HHDH	1,3-DCP	9.1	18.4	1,011.1	54.9
	2,3-DCP	6.7	28.6	522.2	18.3

The concentration of using 1,3-DCP and 2,3-DCP as substrates at ranging from 10 to 200 mM and the activity was measured under the standard assay conditions

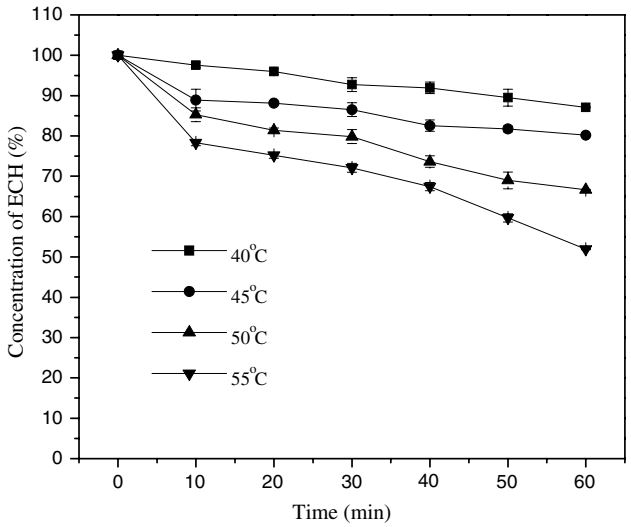

Fig. 8 Effect of temperatures on stability of ECH. Conditions as follows: 20 mM ECH, 0.2 M of Na_2HPO_4–NaH_2PO_4 buffer (pH 7.5) with a final volume of 10 ml, at 40–55 °C for 60 min

(Fig. 10a). The ECH of the reaction mixture was analyzed using a complexation gas chromatography and gas chromatography-mass spectrometry. Mass spectrum of the reaction mixture matches the ECH standard mass spectrum (Fig. 10b), which indicated that the ECH was obtained.

Discussion

HHDH from *A. tumefaciens*, exhibiting high regio- and enantioselectivity toward a range of substrates, has the ability to convert 1,3-DCP to ECH, which is an important C3 compound mainly used as a raw material in the synthesis of fine chemicals and organic chemicals [13, 23, 30].

However, the activity, stability, and tolerance to the high substrate concentration of the HHDH are not satisfactory to be applied to industrial applications. Therefore it is necessary to enhance its performance, especially catalytic

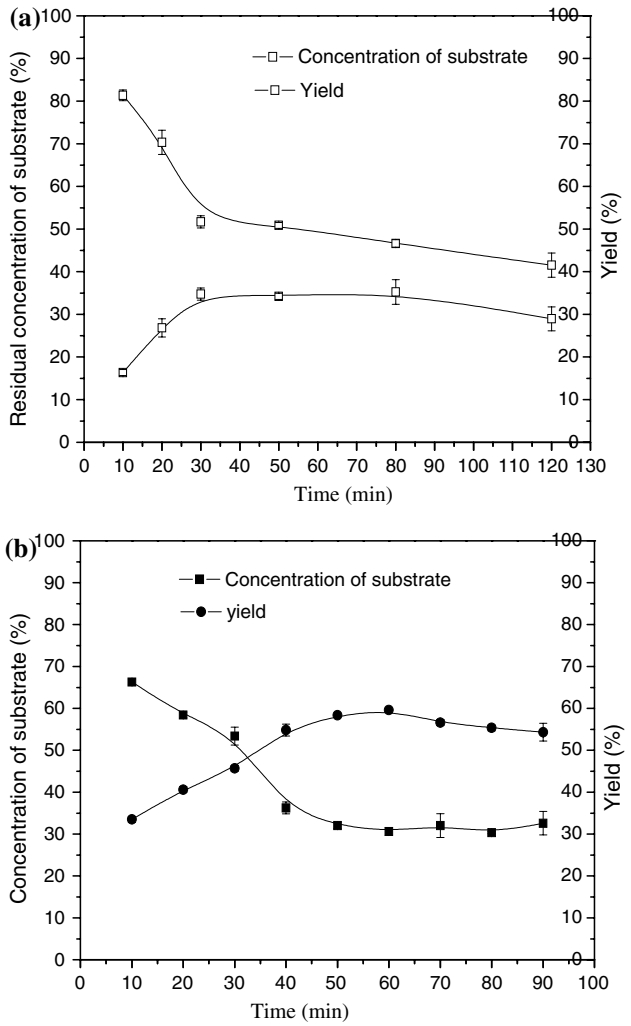

Fig. 9 The conversion time course of 1,3-DCP by HHDH. **a** Wt-HHDH, **b** Mut-HHDH. Reaction conditions for Wt-HHDH: 0.2 M of Na_2HPO_4–NaH_2PO_4 (pH 8.0), 30 mM 1,3-DCP and 211 mg/l Wt-HHDH with a final volume of 10 ml at 45 °C for 1 h. **c** Reaction conditions for Mut-HHDH: 0.2 M $Na_2B_4O_7$–H_2BO_3 (pH 8.4), 100 mM 1,3-DCP and 3.8 mg/l Mut-HHDH with a final volume of 10 ml at 45 °C for 2 h

activity and tolerance to the high substrate concentration in order to meet the requirement of large-scale application [9, 37]. Site-directed mutagenesis, a powerful tool in which a mutation is created at a defined site in a piece of DNA, has been widely used to improve enzyme properties such as catalytic activity, stability, and substrate specificity [26, 34, 36]. In this study, in order to improve catalytic efficiency and stability, HHDH was modified by a sequential site-directed mutagenesis [14, 15, 37]. Based on previous studies and structural analysis of HHDH, and a Mut-HHDH was obtained.

The tertiary structure of Mut-HHDH was obtained by homology modeling and compared with Wt-HHDH. The results showed that the substrate-binding pocket of Mut-HHDH was more open after mutagenesis. This is mainly due to the substitutions in which the residues with the larger side chains was replaced by smaller ones such as Thr131Ala, Thr134Ala, Thr144Ala, and Thr146Ser. Another important contribution to the openness of the substrate-binding pocket is the substitution Trp249Ala, which released a lot of space of active site. According to the polarity of the nature of R-based, Thr is a non-charged polar amino acid, while Ala belongs to non-polar R-based amino acid. Ala is more hydrophobic than Thr, thus it is favorable for the interaction of active site and substrates. In addition, other mutations (Phe, Met, Pro, Trp, and Tyr) are hydrophobic amino acids, which can create an attraction environment for the hydrophobic substrate. Moreover, the molecular docking showed that the orientations of 1,3-DCP in the active sites of Wt-HHDH and Mut-HHDH are different. In the Mut-HHDH, the distance between the hydroxyl of 1,3-DCP and Tyr145 is much closer. Therefore, Tyr145 is easier to abstract proton from the hydroxyl group. Meanwhile, the distance reduction between 1,3-DCP and Ser132 leads to the conformation of a hydrogen bond that can stabilize the substrate in the active site [5, 31]. These changes have played a primary role in increasing the enzyme activity. Previous study has demonstrated that Cys153 is an important residue involved in the enzyme inactivation process [27]. The mutation Cys153Ser prevented the formation of disulfide bonds between Cys153 and Cys229, which is the major contribution to improve the stability of the enzyme. In addition, the Mut-HHDH contains more than five hydrophobic amino acid residues after mutagenesis, which contributed to the enhanced thermostability of the enzyme.

To assess the potential application of Mut-HHDH, the biochemical properties of the purified Mut-HHDH were investigated and compared with that of Wt-HHDH. The specific activity of the Mut-HHDH toward 1,3-DCP was 582 U/mg, approximately 26-fold higher than that of Wt-HHDH (22 U/mg). The value of k_{cat} (1,011.1/s) were enhanced 18.4-fold than the Wt-HHDH (54.9/s). The thermostability of the Mut-HHDH was substantially higher than that of Wt-HHDH. As expected the half-life of the enzyme was increased threefold compared to Wt-HHDH. These improved features are especially desirable in industrial applications. Moreover, the Mut-HHDH showed higher optimal temperature (65 °C) than Wt-HHDH (53 °C), which made it possible for synthesis of some thermally stable compounds and biodegradation of various halogenated pollutants.

In conclusion, a gene encoding HHDH from *A. tumefaciens* was cloned and expressed in *E. coli*. To increase its activity and stability, the Wt-HHDH was further modified by site-directed mutagenesis. The specific activity of the Mut-HHDH was enhanced 26-fold and the value of

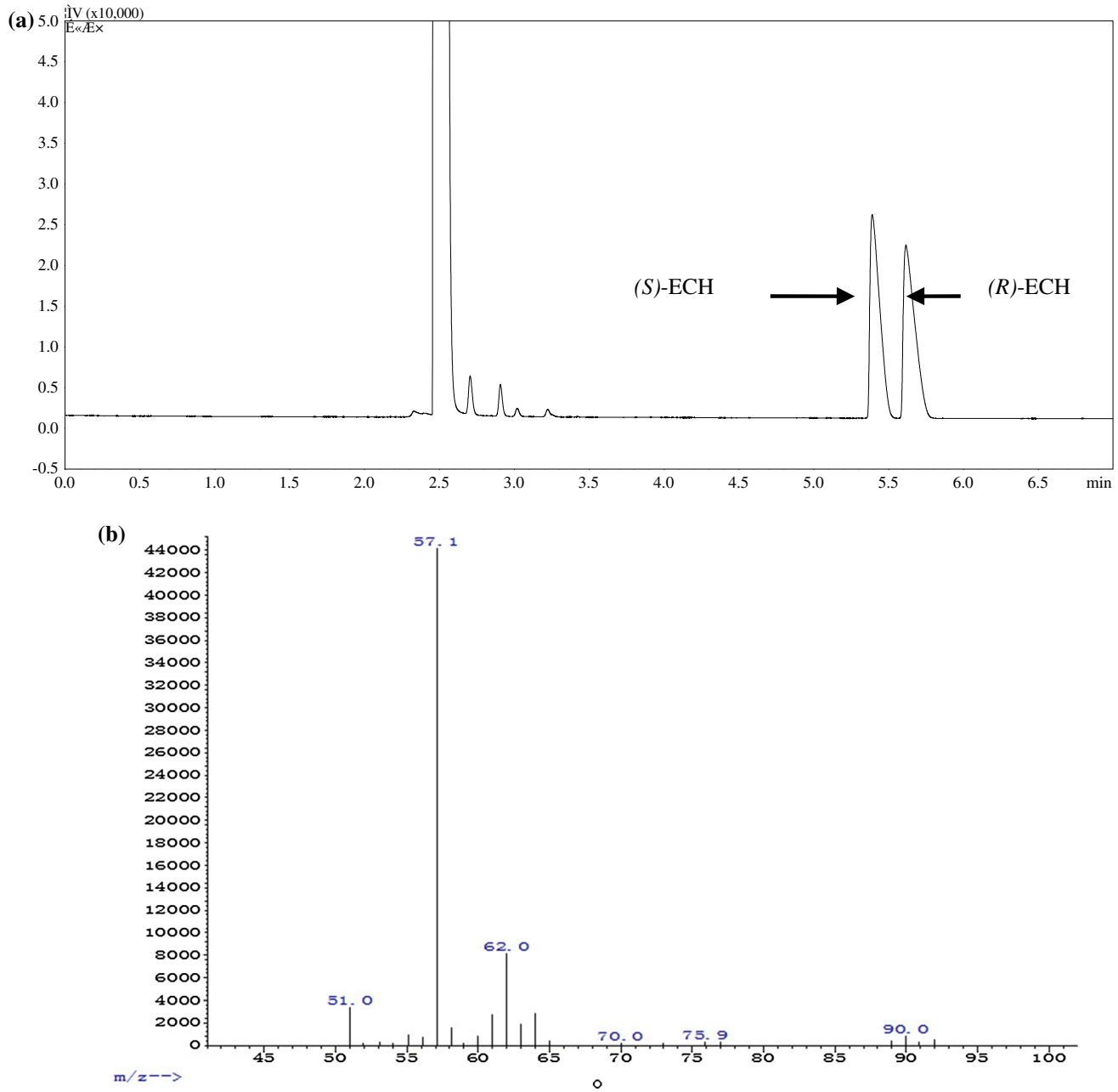

Fig. 10 Analysis of ECH. **a** Estimation of optical purity of (*R*)-ECH and (*S*)-ECH by complexation gas chromatography, and **b** the gas chromatography-mass spectrum of ECH

k_{cat} was 18.4-fold than that of Wt-HHDH, respectively. The Mut-HHDH showed threefold extension of half-life at 45 °C compared to Wt-HHDH. Structure analysis showed that the Mut-HHDH had a more accessible substrate-binding pocket than the Wt-HHDH. After mutation, the distance between the substrate and active site became closer in the mutant compared to Wt-HHDH, which improved the catalytic activity. This Mut-HHDH could be a potential candidate for the production of ECH at an industrial scale.

Acknowledgments This work was financially supported by the National Natural Science Foundation of China (No. 21176224), National Basic Research Program of China (973 Program) (No. 2011CB710806), National Major Project of Scientific Instruments Development of China (No. 2012YQ150087) and the Natural Science Foundation of Zhejiang Province of China (No. Z4080032 and R3110155).

References

1. Archelas A, Furstoss R (1997) Synthesis of enantiopure epoxides through biocatalytic approaches. Annu Rev Microbiol 51(1):491–525
2. Assis HMS, Sallis PJ, Bull AT, Hardman DJ (1998) Biochemical characterization of a haloalcohol dehalogenase from *Arthrobacter erithii* H10a. Enzyme Microb Technol 22(7):568–574
3. Bornscheuer UT, Hesseler M (2010) Enzymatic removal of 3-monochloro-1, 2-propanediol (3-MCPD) and its esters from oils. Eur J Lipid Sci Technol 112(5):552–556
4. Chung CT, Niemela SL, Miller RH (1989) One-step preparation of competent *Escherichia coli*: transformation and storage of bacterial cells in the same solution. Proc Natl Acad Sci USA 86(7):2172–2175
5. de Jong RM, Tiesinga JJW, Rozeboom HJ, Kalk KH, Tang LX, Janssen DB, Dijkstra BW (2003) Structure and mechanism of a bacterial haloalcohol dehalogenase: a new variation of the short-chain dehydrogenase/reductase fold without an NAD(P)H binding site. EMBO J 22(19):4933–4944
6. de Jong RM, Tiesinga JJW, Villa A, Tang LX, Janssen DB, Dijkstra BW (2005) Structural basis for the enantioselectivity of an epoxide ring opening reaction catalyzed by halo alcohol dehalogenase HheC. J Am Chem Soc 127(38):13338–13343
7. DeLano WL (2002) The PyMOL user's manual. DeLano Scientific, San Carlos 452
8. Elenkov MM, Hauer B, Janssen DB (2006) Enantioselective ring opening of epoxides with cyanide catalysed by halohydrin dehalogenases: a new approach to non-racemic β-hydroxy nitriles. Adv Synth Catal 348(4–5):579–585
9. Fox RJ, Davis SC, Mundorff EC, Newman LM, Gavrilovic V, Ma SK, Chung LM, Ching C, Tam S, Muley S (2007) Improving catalytic function by ProSAR-driven enzyme evolution. Nat Biotechnol 25(3):338–344
10. Haak RM, Berthiol F, Jerphagnon T, Gayet AJA, Tarabiono C, Postema CP, Ritleng V, Pfeffer M, Janssen DB, Minnaard AJ (2008) Dynamic kinetic resolution of racemic β-haloalcohols: direct access to enantio-enriched epoxides. J Mol Catal B Enzym 130(41):13508–13509
11. Hasnaoui-Dijoux G, Majerić Elenkov M, Lutje Spelberg JH, Hauer B, Janssen DB (2008) Catalytic promiscuity of halohydrin dehalogenase and its application in enantioselective epoxide ring opening. Chem Biol Chem 9(7):1048–1051
12. Higgins TP, Hope SJ, Effendi AJ, Dawson S, Dancer BN (2005) Biochemical and molecular characterisation of the 2, 3-dichloro-1-propanol dehalogenase and stereospecific haloalkanoic dehalogenases from a versatile *Agrobacterium* sp. Biodegradation 16(5):485–492
13. Janssen DB, Majeric-Elenkov M, Hasnaoui G, Hauer B, Spelberg JHL (2006) Enantioselective formation and ring-opening of epoxides catalysed by halohydrin dehalogenases. Biochem Soc Trans 34(2):291–295
14. Jin HX, Hu ZC, Liu ZQ, Zheng YG (2012) Nitrite-mediated synthesis of chiral epichlorohydrin using halohydrin dehalogenase from *Agrobacterium radiobacter* AD1. Biotechnol Appl Biochem 59(3):170–177
15. Jin HX, Liu ZQ, Hu ZC, Zheng YG (2013) Production of (*R*)-epichlorohydrin from 1,3-dichloro-2-propanol by two-step biocatalysis using haloalcohol dehalogenase and epoxide hydrolase in two-phase system. Biochem Eng J 74:1–7
16. Kalogeris E, Antzoulatos O, Mamma D (2007) Application of different processes for the biodegradation of 1, 3-dichloro-2-propanol by the bacterium *Pseudomonas putida* DSM437. Chem Biochem Eng Q 21(3):297–305
17. Kawthekar RB, Bi W-t, Kim G-J (2008) Synthesis and application of bimetallic chiral [Co(salen)]-type complexes: a new catalytic approach to synthesis of optically pure β-blockers via kinetic resolution of epichlorohydrin. Appl Organomet Chem 22(10):583–591
18. Laemmli UK (1970) Cleavage of structural proteins during the assembly of the head of bacteriophage T4. Nature 227(5259):680–685
19. Liu ZQ, Zhang LP, Cheng F, Ruan LT, Hu ZC, Zheng YG, Shen YC (2011) Characterization of a newly synthesized epoxide hydrolase and its application in racemic resolution of (*R*, *S*)-epichlorohydrin. Catal Commun 16(1):133–139
20. Lutje Spelberg JH, Tang LX, van Gelder M, Kellogg RM, Janssen DB (2002) Exploration of the biocatalytic potential of a halohydrin dehalogenase using chromogenic substrates. Tetrahedron Asymmetry 13(10):1083–1089
21. Majeric Elenkov M, Tang LX, Hauer B, Janssen DB (2006) Sequential kinetic resolution catalyzed by halohydrin dehalogenase. Org Lett 8(19):4227–4229
22. Nagasawa T, Nakamura T, Yu F, Watanabe I, Yamada H (1992) Purification and characterization of halohydrin hydrogen-halide lyase from a recombinant *Escherichia coli* containing the gene from a *Corynebacterium* sp. Appl Microbiol Biotechnol 36(4):478–482
23. Nouailhas H, Aouf C, Le Guerneve C, Caillol S, Boutevin B, Fulcrand H (2011) Synthesis and properties of biobased epoxy resins. Part 1. Glycidylation of flavonoids by epichlorohydrin. J Polym Sci A 49(10):2261–2270
24. Sambrook J, Russell DW, Russell DW (2001) Molecular cloning: a laboratory manual. Cold Spring Harbor Laboratory Press, New York
25. Smith PK, Krohn RI, Hermanson GT, Mallia AK, Gartner FH, Provenzano MD, Fujimoto EK, Goeke NM, Olson BJ, Klenk DC (1985) Measurement of protein using bicinchoninic acid. Anal Biochem 150(1):76–85
26. Tang LX, Torres Pazmiño DE, Fraaije MW, de Jong RM, Dijkstra BW, Janssen DB (2005) Improved catalytic properties of halohydrin dehalogenase by modification of the halide-binding site. Biochemistry 44(17):6609–6618
27. Tang LX, van Hylckama Vlieg JET, Lutje Spelberg JH, Fraaije MW, Janssen DB (2002) Improved stability of halohydrin dehalogenase from *Agrobacterium radiobacter* AD1 by replacement of cysteine residues. Enzyme Microb Technol 30(2):251–258
28. Tang LX, van Merode AEJ, Lutje Spelberg JH, Fraaije MW, Janssen DB (2003) Steady-state kinetics and tryptophan fluorescence properties of halohydrin dehalogenase from *Agrobacterium radiobacter*. Roles of W139 and W249 in the active site and halide-induced conformational change. Biochemistry 42(47):14057–14065
29. Van Den Wijngaard AJ, Janssen DB, Witholt B (1989) Degradation of epichlorohydrin and halohydrins by bacterial cultures isolated from freshwater sediment. J Gen Microbiol 135(8):2199–2208
30. van den Wijngaard AJ, Reuvekamp PT, Janssen DB (1991) Purification and characterization of haloalcohol dehalogenase from *Arthrobacter* sp. strain AD2. J Bacteriol 173(1):124–129
31. van Hylckama Vlieg JET, Tang LX, Spelberg JHL, Smilda T, Poelarends GJ, Bosma T, van Merode AEJ, Fraaije MW, Janssen DB (2001) Halohydrin dehalogenases are structurally and mechanistically related to short-chain dehydrogenases/reductases. J Bacteriol 183(17):5058–5066
32. Yonetani R, Ikatsu H, Miyake-Nakayama C, Fujiwara E, Maehara Y, Miyoshi S, Matsuoka H, Shinoda S (2004) Isolation and characterization of a 1, 3-dichloro-2-propanol-degrading bacterium. J Health Sci 50(6):605–612
33. You ZY, Liu ZQ, Zheng YG, Shen YC (2013) Characterization and application of a newly synthesized 2-deoxyribose-5-phosphate aldolase. J Ind Microbiol Biotechnol 40(1):29–39
34. Yu CL, Parales RE, Gibson DT (2001) Multiple mutations at the active site of naphthalene dioxygenase affect regioselectivity and enantioselectivity. J Ind Microbiol Biotechnol 27(2):94–103

35. Yu F, Nakamura T, Mizunashi W, Watanabe I (1994) Cloning of two halohydrin hydrogen-halide-lyase genes of *Corynebacterium* sp. strain N-1074 and structural comparison of the genes and gene products. Biosci Biotechnol Biochem 58(8):1451–1457
36. Zheng HC, Liu YH, Sun MZ, Han Y, Wang JL, Sun JS, Lu FP (2013) Improvement of alkali stability and thermostability of *Paenibacillus campinasensis* family-11 xylanase by directed evolution and site-directed mutagenesis. J Ind Microbiol Biotechnol 41(1):153–162
37. Zou SP, Du EH, Hu ZC, Zheng YG (2013) Enhanced biotransformation of 1,3-dichloro-2-propanol to epichlorohydrin via resin-based in situ product removal process. Biotechnol Lett 35(6):937–942